MAGNETIC MEASUREMENTS OF PERMANENT MAGNET INSERTION DEVICES AT THE BNL-NSLS

L.Solomon, G.Decker, J.Galayda,

National Synchrotron Light Source

Brookhaven National Lab, Upton, New York 11973

M. Kitamura

Hitachi Research Laboratory, Hitachi Ltd., Japan

Since June 1988, three permanent magnet insertion devices of the hybrid type have been installed into the X-Ray ring at the National Synchrotron Light Source at Brookhaven National Lab as part of the Phase II facility upgrade. The three magnets consist of a soft x-ray undulator (SXU) and two hybrid wigglers, with peak fields of 0.35 and 1.2 Tesla respectively.

The SXU magnet has iron poles, samarium cobalt permanent magnets, 80mm period length, 77 poles, and a gap range of 31 - 100mm. For this gap range the undulator parameter K, where K = 0.934 B(Tesla) λ(cm), ranges from 2.6 to 0.15. The hybrid wigglers have vanadium permendur poles, samarium cobalt magnets, 120mm periods, 31 poles, and a gap range of 22 - 122mm. For this gap range K ranges from 13.0 to 0.5. All three of these magnets have electromagnetic coils which can be powered to adjust the value of the magnet field integral. Both point and integral magnetic measurements were performed on these magnets; some of the measurement results will be presented in this paper.

The relative strength of the individual magnets was measured in a Helmholtz coil, where the integrated voltage generated as the block slides down a chute is directly proportional to the magnetic strength. In this manner the magnitude of two of the three orthogonal components of the magnetization, M_z and M_y, were measured for each block; typically $M_y/M_z \leq 2\%$. A coordinate system is defined so that $\hat{z}$ is along the electron beam direction, $\hat{y}$ is the axis orthogonal to the plane of the poles, and $\hat{x}$ is the axis which is both along the poles and orthogonal to the electron beam direction. In the assembled undulator the *major* magnetization, M_z was oriented along $\hat{z}$, and the *minor* component M_y, was along $\hat{y}$. To help determine specifically where the individual magnets should be located in the magnet halves, the magnetic field at the midplane of the undulator due to a single block (the *transfer function*) was measured prior to assembly of the two magnet halves. For example, in the SXU magnet, which has two magnets per slot, the transfer function was measured for a single block in the *high* position (closer to the magnet midplane) and *low* position (farther from the magnet midplane) in a magnet half, and for M_z oriented along $\hat{z}$ and along $\hat{y}$. To measure the *major* transfer function M_z was oriented along $\hat{z}$, and a steel plate was held over the magnet half. The plate set the boundary conditions and imposed midplane symmetry. In order to measure the *minor* transfer function an empty beam was used in place of the steel plate. The effect of a minor component along $\hat{x}$ has been measured and is ≈ 10% of that due to the minor component along $\hat{y}$. Clearly, measurement of these transfer functions makes accessible the determination of vertical steering effects. Transfer functions are plotted for the SXU magnet in Figure 1. The first and second integrals associated with these fields are plotted in Figures 2 and 3 respectively. A notable feature of this data is that the integrated effect of the minor component of the magnet block further from the midplane is greater than that of the magnet nearer the midplane, though the magnitude of the midplane field is more strongly affected by the block nearer the midplane. In the X21 and X25 magnet, where there are 8 magnets per slot arranged in 4 layers, the layers nearest and furthest from the electron beam contribute more strongly to the midplane field integrals than the middle two layers.

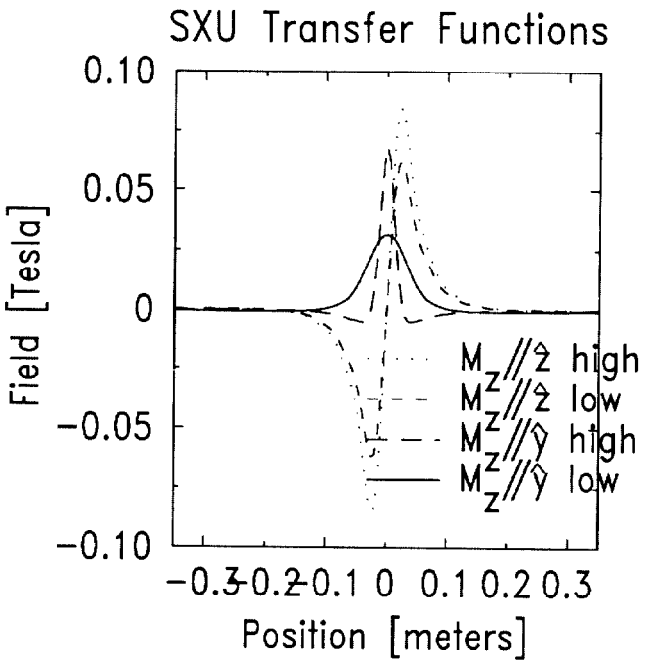

Figure 1 - The measured single block transfer functions in the SXU

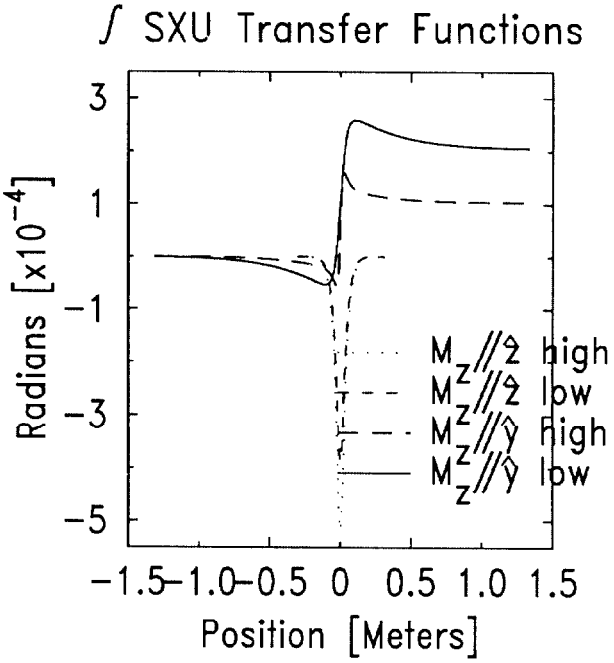

Figure 2 - The first integral of the single block transfer functions shown in Figure 1.

CH2669-0/89/0000-0387$01.00©1989 IEEE

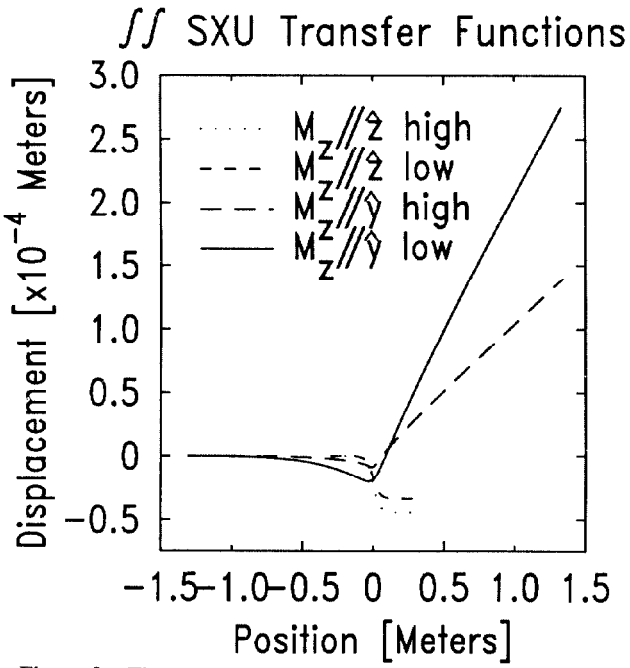

Figure 3 - The second integral of the single block transfer functions shown in Figure 1.

Transfer functions were used to determine the placement of the magnet blocks in the magnet beams. The optimal arrangement of magnet blocks minimizes the first and second integrals of the magnetic field, which are directly related to the angular deviation, Θ, and the linear displacement, X, respectively of the electron beam upon emerging from the insertion device i.e.

$$\Theta \approx \frac{1}{B\rho} \int_0^L B(z')dz'$$

$$X \approx \frac{1}{B\rho} \int_0^L dz \int_0^z B(z')dz'$$

where $B\rho$, the magnetic rigidity, is 8.3391 Tesla meters at 2.5 GeV, and L is the magnet length.

Hall probe data taken on the insertion magnets as a function of gap is integrated to obtain Θ , and may be compared to data obtained from long coil measurements. The long coil measurements are made with two coils which are 90° apart and which are supported on a G10 tube. Each coil is a diameter coil which is wound with a 20 strand wire. The tube is rotated 180° and the integrated voltage, which is proportional to the change in the magnetic flux cutting the coil, is read. The tube is oriented so that initially one of the coil windings is in the horizontal plane, which allows measurement of the integrated B_y, and the other coil is initially in the vertical plane, allowing measurement of B_x. The agreement between the long coil and the hall probe results is very good; e.g. in the SXU the difference in the integral was ≈ 0.2 Gauss-meters over 4 meters, a fraction of the integral due to the earth's field.

The angular displacement Θ as obtained by numerical integration of the Hall probe data is shown for the SXU magnet gaps of 31,50,and 90mm in Figure 4 at the operating currents of the end correctors (I= 0.65, 3.2, and 4.6 respectively). For clarity, the 50 and 90mm trajectories are displaced by 1.0 and 2.0 $\times 10^{-3}$radians, respectively, from the 31mm trajectory. Figure 5 shows the trajectory at magnet gaps of 31, 50, and 90mm at the operating currents of the end correctors. For clarity the 50 and 90 mm trajectories are displaced by 0.2 and 0.4 $\times 10^{-4}$ meters, respectively, from the 31 mm trajectory.

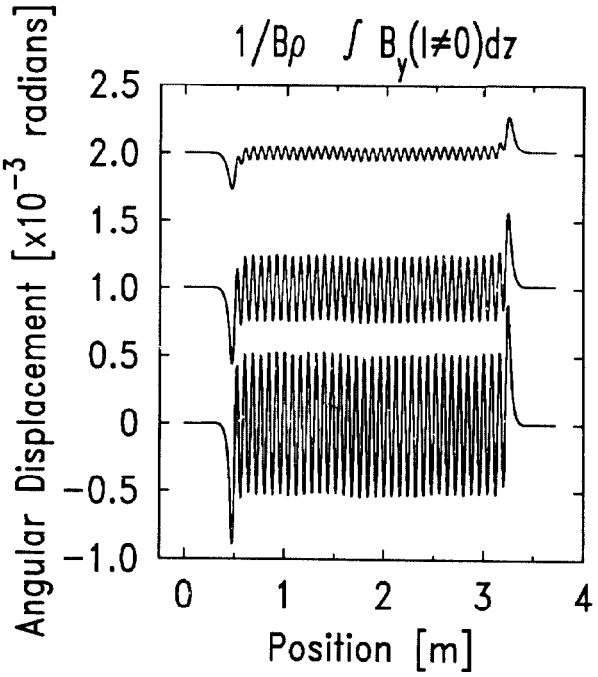

Figure 4 - SXU hall probe data is integrated to obtain the angular deviation of the electron beam. Shown is data at gaps of 31,50,and 90mm at the operating currents of the end correctors (I= 0.65, 3.2, and 4.6 respectively). For clarity, the 50 and 90mm trajectories are displaced by 1.0 and 2.0 $\times 10^{-3}$radians, respectively, from the 31mm trajectory.

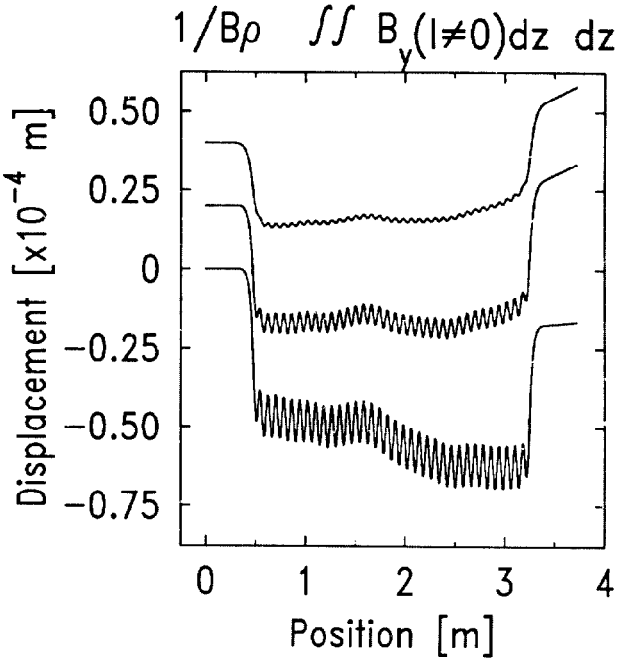

Figure 5 - SXU hall probe data is integrated twice to obtain the trajectory at magnet gaps of 31, 50, and 90mm at the operating currents of the end correctors. For clarity the 50 and 90 mm trajectories are displaced by 0.2 and 0.4 $\times 10^{-4}$ meters, respectively, from the 31 mm trajectory.

Long coil data obtained on the SXU yielded both the integrated B_y and B_x. B_y causes the beam to oscillate in the horizontal plane, and B_x causes the beam to oscillate in the vertical plane. Figures 6 and 7 show the integrated B_y and B_x, respectively, as a function of position X and gap at zero end corrector current.

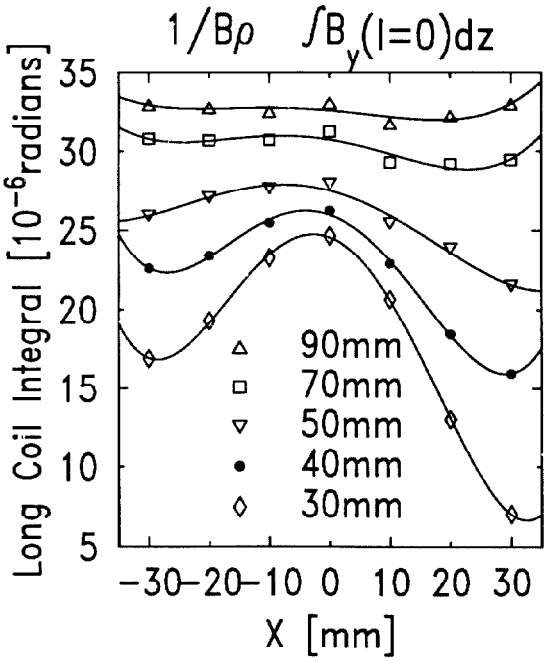

Figure 6 - SXU long coil data for B_y as a function of position X and gap.

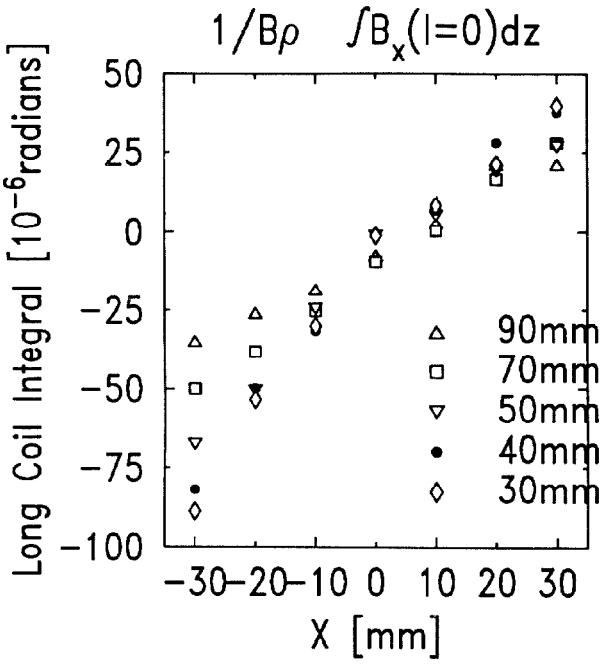

Figure 7 - SXU long coil data for B_x as a function of position X and gap.

The long coil measurements of the X21 and X25 magnets are presented in Figures 8 and 9, and show the integrated B_y and B_x as a function of gap.

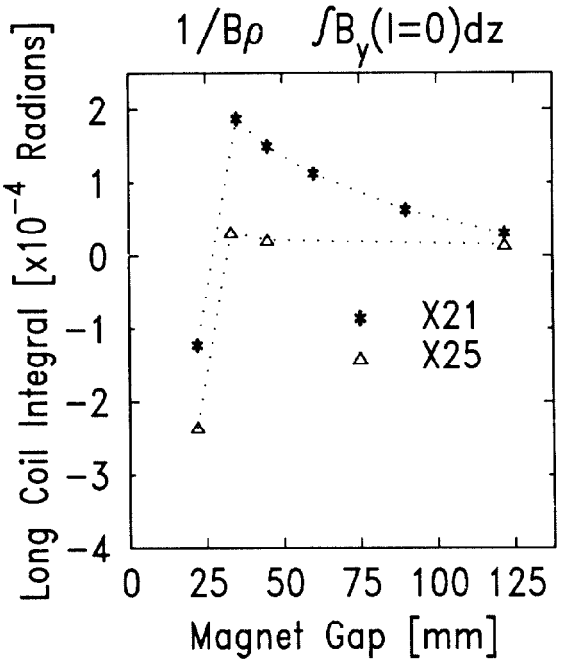

Figure 8 - X21 and X25 long coil data for B_y.

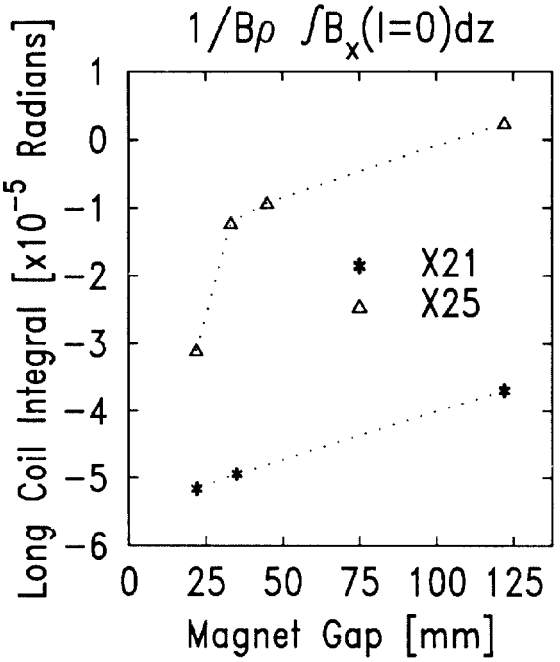

Figure 9 - X21 and X25 long coil data for B_x.

A more inclusive summary of our magnetic measurement results is being prepared and will be ready for publication shortly.

This work has been supported under the auspices of the U.S. Department of Energy. The authors wish to acknowledge helpful private communications with K.Halbach and B.Kincaid.